Article

Chinese Science Bulletin

Sun & Solar System

September 2012 Vol.57 No.25: 3375–3380
doi: 10.1007/s11434-012-5365-y

Spectra of L-band ionospheric scintillation over Nanjing

FANG HanXian[1,2], YANG ShengGao[1,2*] & WANG SiCheng

[1] *Institute of Meteorology, PLA University of Science and Technology, Nanjing 211101, China;*
[2] *State Key Laboratory of Space Weather, Chinese Academy of Sciences, Beijing 100190, China*

Received January 6, 2012; accepted March 19, 2012

We report the spatiotemporal statistical characteristics of amplitude scintillation over Nanjing. A FFT method for computing scintillation intensity power spectra is briefly described. Using this method, the data with ISATM in Nanjing is analyzed. Spectra characteristic is presented and the irregularities property is discussed preliminarily. The results reveal that the power spectra obtained for Nanjing is consistent with theoretical modeling. At frequencies below the Fresnel frequency, the power density plotted on log-log scale is almost constant whereas above it asymptotes to a straight line. The spectral index ranges from 1.71 to 1.92, which has positive correlation with the S_4 index. Finally, the average drift velocity of irregularities is computed assumably and compared with that obtained for Xinxiang and Haikou.

ionospheric scintillation, scintillation power spectra, electronic density irregularity, spectra index

Citation: Fang H X, Yang S G, Wang S C. Spectra of L-band ionospheric scintillation over Nanjing. Chin Sci Bull, 2012, 57: 3375–3380, doi: 10.1007/s11434-012-5365-y

The ionosphere often features irregularities resulting from various unstable turbulence processes. When a radio wave from an extraterrestrial source, such as an artificial satellite, passes through the ionosphere, its wavefront will be distorted by the inhomogeneity present in the ionospheric plasma. As a result, the amplitude and phase of signals fluctuate, and the scintillation can be observed [1]. On propagating to the ground, these amplitude and phase variations cause interference to occur resulting in a diffraction pattern. Severe scintillations negatively affect trans-ionospheric radio communications and can interrupt or degrade GPS receiver operation by causing fading of the in-phase and quadrature signals, making the determination of phase by a tracking loop impossible. Degradation occurs when phase scintillations increase the frequency of cycle slips on the phase, and thus introduce ranging errors which in turn increase the dilution of precision and reduce the accuracy of GPS navigation. Since ionospheric scintillation originates from random electron density irregularities acting as wave scatterers, research on the formation and evolution of irregularities is closely related to scintillation studies [2]. A large number of theoretical investigations and statistical results have shown that the spectral analysis of scintillations from discrete radio sources and artificial satellites provides a new and valuable technique for investigating the continuous spectrum of small scale electron density irregularities in the ionosphere [3]. Information about irregularities in velocity, the equivalent thickness of the scattering layer, and irregularities in electron density can be deduced using conventional diffraction theory [4]. Also, knowledge of these irregularites is important in understanding the physical mechanisms underlying their formation and evolution; this is crucial in scintillation modeling [2].

During the past few decades, theoretical models have been developed to explain scintillation and provide equations for use in predicting. The theoretical models generally depend upon an assumption about the shape of the power spectrum of electron density fluctuations along the path. Thus observations of power spectrum of electron density have been of interest to some scholars [3,5–9], with many excellent reviews on this subject being published. Using VHF beaconing, Basu [10] found that the scintillation power

*Corresponding author (email: yangshenggao198759@163.com)

spectra index is from −3 to −4.5 near the equatorial region, and the irregularity scale is less than 1 km. Kerslcy [11] analyzed the data of VHF signal receiver over high-latitude region, revealing that the index is from −2.5 to −4.5, the irregularity scale is from 150 m to 1 km. Observations on the scintillation of VHF signals at Xinxiang [4] showed "break out" in the power spectra, and the power spectra index has positive correlation with the scintillation index S_4.

This paper presents the spatiotemporal statistical characteristics of amplitude scintillation and reports results from an analysis of the Fourier power spectrum of ionospheric scintillation data over Nanjing. The spectral characteristics are presented and some properties of irregularities for this region are discussed preliminarily.

1 Data and algorithm

1.1 Data

The data was recorded at Nanjing (31.97°N, 118.81°E) using GPS satellites as sources. The direct observations require the use of dedicated GPS ionospheric scintillation and total electron content monitors (GISTM), such as the GSV4004B (Novatel/GPS Silicon Valley), which records the amplitude and phase of the L1 (1.57542 GHz) and L2 (1.2276 GHz) frequencies in the GPS signals at a rate of 20 Hz under computer control as well as several scintillation-related parameters. Such receivers have 48 channels, can track 24 satellites simultaneously (12 GPS satellites and 12 GLONASS satellites). It acquire carrier-to-noise ratio (C/N_0) data with the sample rates 20 Hz, and then do some pretreatment with the original data before saving them in data files.

Amplitude scintillations are obtained by monitoring the index S_4. This index is derived from detrended signal intensity of signals received from GPS satellites. The S_4 index, which includes the effects due to ambient noise, is defined as the normalized root mean square of the power P divided by the average power P as follows:

$$S_4 = \sqrt{\frac{\langle P^2 \rangle - \langle P \rangle^2}{\langle P \rangle^2}}, \tag{1}$$

where < > represents the average values over a 60-second interval. Because of the special equipment, the power P cannot be obtained, so it is replaced with a value $10^{CN_0/10}$ from which S_4 can be computed using eq. (1).

We have analyzed the amplitude scintillation statistical characteristic during the period between November 2008 and October 2009 [12] and summarized the results in Figures 1 and 2. Figure 1 is the daily variation of the occurrence rate of the day- and night-time amplitude scintillation intensities (the x-axis refers to the date, and the y-axis is daily scintillation occurrence rate); the percentage of occurrence is computed from the ratio between the total number of observations of some period with defined intensity scintillation (S_4>0.2 or S_4>0.1) to the total number of observations during the whole period [1]. This is the standard method to analyze the occurrence of ionospheric irregularities that cause scintillations in the GPS satellite signals. The amplitude scintillations were rather quiet with scintillation activities with S_4>0.2 occurring infrequently. Different intensities of amplitude scintillation have common spatiotemporal variation characteristics. The occurrence rate in June, August, September and October is higher than that in other months; the highest rate took place in October whereas the lowest was in November. Figure 2 shows the spatial distribution, in polar coordinates, of the occurrence rate of different intensity of amplitude scintillation. The length of the radius vector denotes the elevation of GPS satellite scintillation, and the azimuth of the radius vector is the GPS satellite's azimuthal angle. Color coding is determined from the ratio between the occurrence number of amplitude scintillation

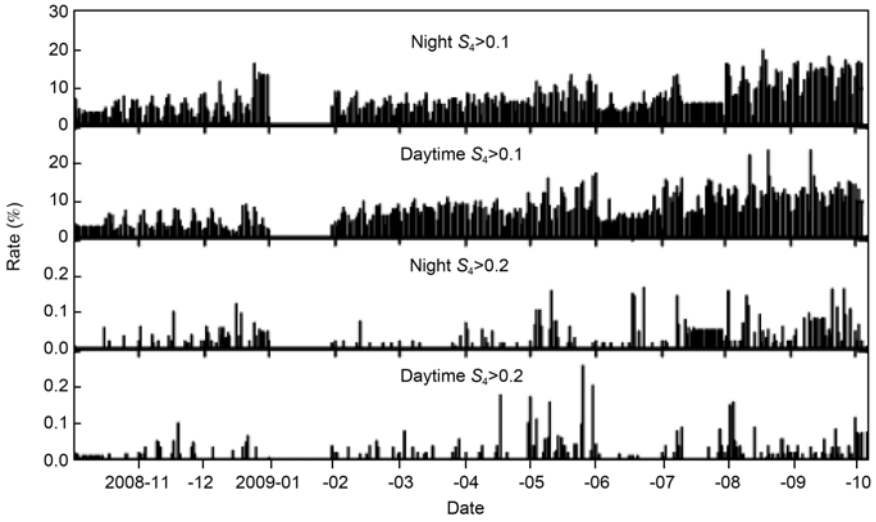

Figure 1 Variation of the occurrence rate in day- and night-time amplitude scintillation intensities [12].

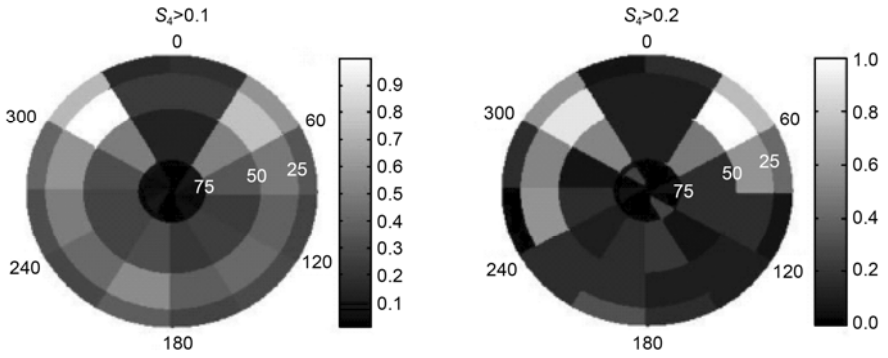

Figure 2 Spatial distribution of the occurrence rate in different amplitude scintillation intensity [12].

in the region to the maximum number of amplitude scintillation. From Figure 2, we can know that most of the scintillation activities took place with elevation 0°–50°, and the occurrence rate in the northern direction is higher than that in the southern direction; this maybe results from high-latitude irregularities drifting to mid-latitude. This conclusion needs more data to support.

In this paper, FFT (Fast Fourier Transform) methods have been used to compute scintillation intensity power spectra using the original carrier-to-noise data. According to [4], the best length of serial data is 2^n (n a positive integral number), therefore choosing 2048 (approximately 102 seconds) dots to compute the power spectra. To eliminate the influence of low elevation, data associated with elevations lower than 30° are discarded. Since the original data include not only the useful disturbance information, but also the background trend and high-frequency noise, picking out the disturbance information is the first step in processing data. The original data is used to obtain a straight line fit by the least-squares method, then using the original serial data to subtract the straight-line serial data. This results in detrended serial data which is finally transformed into a Fourier power spectra using the Welch algorithm [13].

1.2 Welch algorithm

Based on the discrete Fourier transform, the classical method of spectrum estimation implies windowing the infinite data sequence. Consequently, it has some disadvantages such as low resolution. To overcome these disadvantages, some improved algorithms are provided, such as Barlett algorithm, Welch algorithm, Nattal algorithm. The Welch algorithm is a modified method for periodograms. As outlined in Figure 3, the Welch algorithm is made up of four steps. First, the time serial data is partitioned into m (m is a positive integral number) segments of the same length. Every segment will be processed with a window function (Hamming Window, Rectangular Window), and then with each a power spectrum is computed. Finally, the mean of all the results gives the final power spectrum.

2 Theoretical and computed power spectra

2.1 Simulation of GPS scintillation spectra

The theory of ionospheric scintillation is based on the propagation and scattering theory of electromagnetic waves in ionospheric random medium. Under weak fluctuation conditions, the phase screen theory and Rytov approximation are frequently applied. In weak scattering theory, there is an assumption that the irregularity is associated with an isotropic stationary field. Expanding the spatial wavenumber spectra of the scintillation signal, the monostatic signal intensity spectra expression can be written as

$$\Phi_I(f) = \frac{\lambda^2\sigma_\xi^2 L k_p{}^4 R_0^3 \Gamma(p/2)}{\pi\nu\cdot\pi^{3/2}\Gamma\left(\frac{p-3}{2}\right)} \int_0^\infty \frac{\sin^2\left[\frac{\lambda z}{4\pi}\left(\kappa_x^2+\kappa_y^2\right)\right]}{\left[1+R_0^2\left(\kappa_x^2+\kappa_y^2\right)\right]^{p/2}} \mathrm{d}\kappa_y;$$
$$\kappa_x = 2\pi f / v, \tag{2}$$

where λ is the wavelength, σ_ξ standard deviation of the fluctuation variance of electron density, p spectra index, z the mean height of the scattering layer, κ_x and κ_y are the spatial wavenumber components in directions x and y respectively, v is the irregularity drift velocity, L the equivalent thickness of the irregularity, R_0 related to the outer scale, f frequency, and Γ the Gamma function. Abundant studies suggest that the ionospheric scintillation power

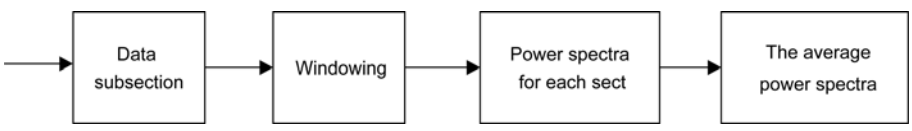

Figure 3 Flowchart of power spectrum estimation using the Welch method.

spectrum shows a power-law relationship at high frequency, which means Φ_I is proportional to f^{-n} (n=–p–1). Plotting 10log$f$ along the x-axis, and 10log(Φ_I) along the y-axis, the graph in Figure 4 is the theoretical numerical FFT spectra of L-band scintillation. In log-log scale, the spectra is smooth at low frequency, but decreasing asymptotically to a straight line with increasing frequency; this behavior corresponds to $\Phi_I \propto f^{-n}$. If using the least-squares straight line fit at high frequency, the straight slope k and n have relationship k=n as indicated by the right arrow. As n increases further, the straight line decreases faster, and signal fluctuations are more obvious, yielding stronger scintillation. As seen in Figure 4, there are many extremums at high frequencies, which is determined by the Fresnel oscillating function [14]. The frequencies of the minimum spectra density are computed with the following formula [15]:

$$f = \sqrt{n} \cdot v / \sqrt{\lambda z},\ n = 1,\ 2,\ 3, \ldots \quad (3)$$

where v is the drift velocity of the irregularity, λ the radio wave length, and z the height of the irregularity. All frequencies were calculated from eq. (3). For n=1, f is approximately the Fresnel frequency, as marked by the left arrow ($f_{\min}$) in Figure 4 that corresponds to the first Fresnel scale. From eq. (3), if a Fresnel frequency is reached, the irregularity drift velocity can be calculated approximately with

$$v \approx \sqrt{\lambda z} f_{\min}. \quad (4)$$

2.2 Computed spectra

As Nanjing is in the mid-latitude region, ionospheric scintillations are weak most of time; medium to strong scintillations occur rarely. In the data used this paper, those scintillation events with an average S_4 of more than 0.15 are chosen to compute the power spectra. There are 52 events in all: 20 nighttime and 32 daytime.

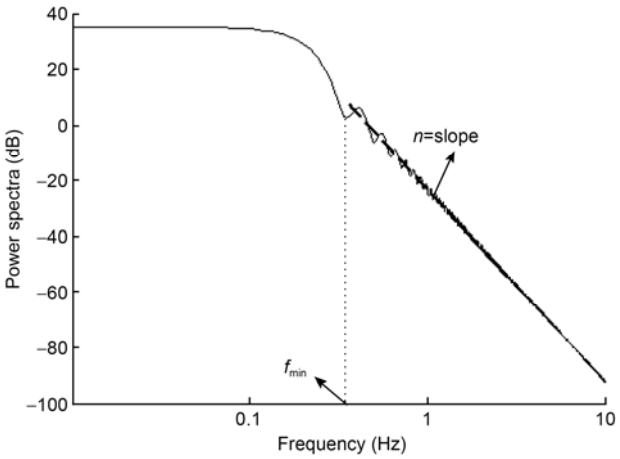

Figure 4 The theoretical spectra for GPS scintillation.

The power spectrum can improve our understanding of the nature and causes of the F-region irregularities. Figures 5 and 6 are classical GPS scintillation intensity power spectra at nighttime and daytime over Nanjing; the x-axis records the log scale of frequency, and y-axis the intensity power. In these semi-logarithmic plots, the power density is almost constant at low frequencies, but decrease at high frequencies with an approximate power-law relationship. These are consistent with the theoretical simulations. The thick straight

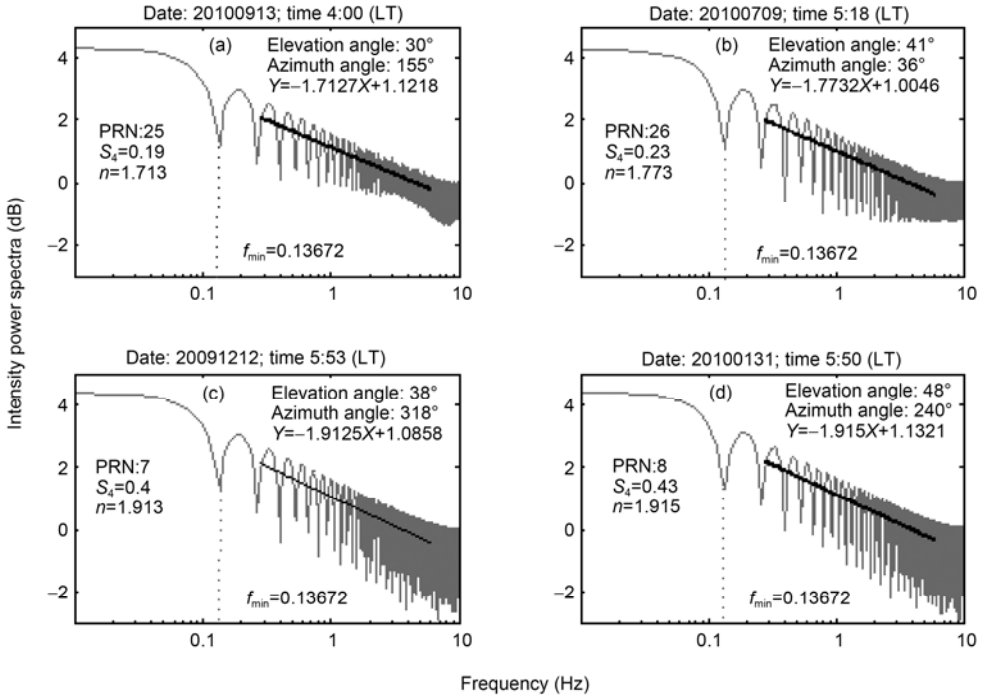

Figure 5 The observed nighttime power spectra of GPS scintillation from different satellites over Nanjing.

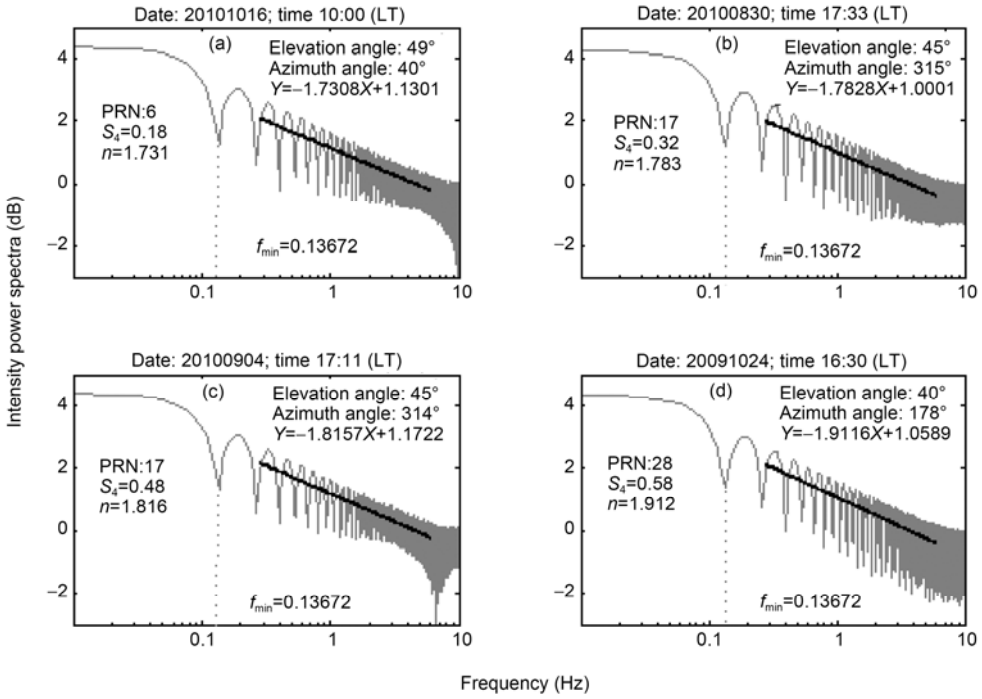

Figure 6 The observed daytime power spectra of GPS scintillation from different satellites over Nanjing.

lines are results fitted from the high frequency spectra, the fitted equations are displayed as inserts beside each line; the slopes are spectral indexes n. From each pair of panels (a)–(d) of Figures 5 and 6, we find that with increasing amplitude scintillation index S_4, the spectral index n varies with the same trend regardless of daytime or nighttime. The frequency ($f_{\min}$) of the first minimum is called the Fresnel frequency since it corresponds in the frequency domain to the Fresnel radius in the spatial domain. Just as there can be essentially no interference, i.e. no intensity fluctuations or scintillations, arising from structure larger than the Fresnel radius (under conditions of weak scattering), so there should be no fluctuations with frequencies less than Fresnel frequency; the Fourier power spectrum should be flat at these low frequencies. All the scintillation events above have the same Fresnel frequency, that is, approximately 0.137 Hz. Moreover, there is a break at high frequencies for some scintillation events, such as Figure 5(a), (b), (c) and Figure 6(a), (b).

Usually in scintillation studies, the fluctuations are characterized by the scintillation index for which the properties can be related to those of the ionospheric irregularities by the application of diffraction theory. The use of the power density spectrum of the intensity fluctuations at an observing point on the ground as a means of studying the irregularities has also drawn attention. Figure 7 shows the amplitude scintillation index S_4 varying with spectra index n using the above-mentioned 52 high-S_4 scintillation events. The two parameters have positive correlation as observed from the fitted straight line and equation. Comparing Figure 7(a) with (b), the scintillation index S_4 in the daytime is larger than at nighttime, but the slope for nighttime data is greater,

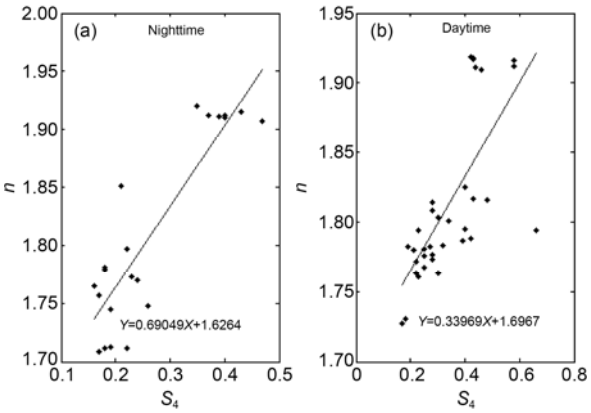

Figure 7 Correlation between S_4 and n at (a) night-times and (b) day-times.

implying that the spectral index n varies faster with scintillation index S_4 at nighttime (0.7) than during the daytime (0.3). No significant difference between the day- and nighttime spectral indices was observed; p is from –2.71 to –2.92 with an average of –2.8.

Through analyzing structures of the 52 power spectra, the averaged Fresnel frequency is 0.137 Hz, assuming an averaged height of the irregularity of 400 km. From eq. (3), the ionospheric irregularities drift velocity in Nanjing can be estimated, that is 37.8 m/s, which is in agreement with the observed values from data recorded at Xinxiang [4].

3 Results and discussion

Having analyzed the statistical characteristics of amplitude

scintillation with data from November 2008 to October 2009, then applied FFT methods and computed the power spectra of the 52 high-S_4 scintillation events, we can finally discuss the properties of the irregularities. The results are as follows.

(1) In low solar activity years, the amplitude scintillations were quite quiet and scintillation activities with S_4> 0.2 occurred infrequently over Nanjing region; the scintillation occurrence rates in June, August, September, and October are higher than from other months; the highest occurrence rate took place in October and the lowest in November. Occurrence rates in northerly directions were higher than those in southerly directions.

(2) At frequencies below the Fresnel frequency the power density is almost constant. At frequencies higher than the Fresnel frequency, the spectrum, as plotted on log-log scales, asymptotes to a straight line corresponding to a dependence $\Phi_I \propto f^{-n}$. This is consistent with theoretical numerical simulation, and signifies that phase screen theory is applicable in weak fluctuation regimes. Also it reflects typical mid-latitude scintillation characteristics.

(3) The spectral index p ranges from 2.72 to 2.92, and increases with S_4; the signal fluctuation which is determined by spectra density is reflected in S_4 values.

(4) An averaged Fresnel frequency of 0.137 Hz was obtained, and a preliminary irregularity velocity of 37.8 m/s calculated. These values are consistent with the result from Xinxiang [4], but not with Haikou [15]. We suggest that the scintillation characteristics over mid-latitude regions are different from those over equatorial regions.

With regard to the scintillation mechanism at mid-latitude, different views have been expressed [16–22], with some believing that it is due to expansions in the equatorial or high-latitude irregularity; others consider sporadic-E (Es) and spread-F are responsible. MacDougall reports [16] that the mid-latitude nighttime irregularities are in the form of north-south sheets. The irregularities appear to be created during evening hours and then tend to last throughout the night until they are washed out by sunlight ion production in the morning. An irregularity production mechanism that seems to work at mid-latitudes and produces sheet-like irregularities is the Perkins instability. The north-east electric field direction in the mid-latitude evening is the direction that Perkins shows as being suitable for the Perkins instability to occur [17]. Sheet-like irregularities that are orientated such that the normal to the sheets is between east and the electric field direction will be amplified by his mechanism. But Kelley [18] view that the mid-latitude E-region irregularities are primarily due to the neutral wind rather than electric fields [19].

Due to limited data events, the scintillation mechanism of Nanjing has not been established, requiring more data for a detailed analysis.

This work was supported by the National Natural Science Foundation of China (40505005) and the Specialized Research Fund for State Key Laboratories.

1 Yeh K C. Radio wave scintillations in the ionosphere. Proc IEEE, 1982, 70: 324–360
2 Wernik A W, Secan J A, Fremouw E J. Ionospheric irregularities and scintillation. Adv Space Res, 2003, 31: 971–981
3 Rufenach C L. Power-law wavenumber spectrum deduced from ionospheric scintillation on observations. J Geophys Res, 1972, 77: 4761–4771
4 Long Q L. The spectra of ionospheric scintillation at Xinxiang. Chin J Radio Sci, 1994, 9: 60–65
5 Crane R K. Spectra of ionospheric scintillation. J Geophys Res, 1976, 81: 2041–2050
6 Basu S, MacKenzie E M, Basu S, et al. 250 MHz/GHz scintillation parametersin the equatorial, polar, and auroral environments. IEEE Select Areas Commun, 1987, SAC-5: 102–115
7 Terence J E. Measurement and interpretation of power spectrums of ionospheric scintillation at a sub-auroral location. J Geophys Res, 1969, 74: 4105–5115
8 Bramley E N. Mid-latitude ionospheric scintillation of geostationary satellite signals at 137 MHz. J Atmos Terr Phys, 1978, 40: 1247–1255
9 Singleton D G. Power spectra of ionospheric scintillation. J Atmos Terr Phys, 1974, 36: 113–133
10 Basu S. Equatorial scintillation—A review. Atmos Terr Phys, 1981, 43: 473–489
11 Kersly H C. Power spectra of VHF intensity scintillations from F2 and E region ionospheric irregularities. J Atmos Terr Phys, 1984, 46: 667–672
12 Yang S G, Fang H X, Weng L B, et al. Preliminary statistic analysis of L-band ionospheric scintillation over Nanjing region in China. Chin J Space Sci, 2011, 31: 765–770
13 Yi X, Qu A H. Matlab simulation analysis of power spectrum estimation based on Welch method (in Chinese). Mod Electr Tech, 2010, 33: 7–9
14 Li J H. Ionospheric scintillation and research on the inversion method of irregularity parameters (in Chinese). Doctoral Dissertation. Xi'an: Xidian University, 2006
15 Ma B K. Ionospheric scintillation spectra and the inversion of the irregularity drift velosity. Chin J Radio Sci, 2010, 25: 779–783
16 MacDougall J, Eadic D C. The shape of midlatitude scintillation irregularities. J Atmos Terr Phys, 2005, 67: 931–935
17 Kagan L M, Kelley M C. A wind-driven gradient drift mechanism for mid-latitude E-region ionospheric irregularities. Geophys Res Lett, 1998, 25: 4141–4144
18 Kelley M C. The Earth's Ionosphere: Plasma Physics and Electrodynamics (International Geophysics Series). San Diego, CA: Academic Press, 1989
19 Basu B. On the linear theory of equatorial study of the wind field effect on the growth and observations. J Geophys Res, 2002, 107: 1199–1208
20 Shang S P, Shi J K, Guo S J. Ionospheric scintillation monitoring and preliminary statistic analysis over Hainan region (in Chinese). Chin J Space Sci, 2005, 25: 23–28
21 Shang S P, Shi J K, Guo S J. Morphological study of L-band ionospheric scintillation in the equatorial region (in Chinese). Chin J Radio Sci, 2006, 21: 410–415
22 Aarons J. 50 Years of radio-scintillation observations. IEEE Aatennas Propagat Mag, 1997, 39: 7–12